Fitting the pair potentials for molten salts: A review in brief

Dmitry Zakiryanov [a] [*]

In vitro and *in silico* studies should supplement each other in order to obtain reliable and comprehensive data on the physicochemical properties of molten salts. To attain the aim, the appropriate simulation technique is needed. Because of the computational speed that classical molecular dynamics could deliver, this method is often the most suitable for calculation of the transport properties. The accuracy of the calculation is of a high degree depending on parameters of the potential. In this paper, we review the basics of the pair potential fitting procedure. As an example, a molten lithium chloride is considered. The comparison of different pair potentials in terms of potential energy and per-atomic forces is performed, with the reference data were obtained by means of the density functional theory. Among the macroscopic properties, the melting temperature and viscosity are calculated.

1. Introduction

The simulation methods interpret and supplement the experimental results. The theoretical approaches are especially relevant in the case of molten salts, because some of *in vitro* studies are challenging due to the aggressive media, toxicity, or extreme conditions.

To model a melt, numerous approaches have been developed. In general, the models suitable for the molecular dynamics simulations can be divided into the three groups:

1) Analytical (classical) potentials
2) *Ab initio* methods
3) Machine learning methods

Let us consider the basic concepts of these methods, as well as their limits of applicability.

Within the concept of analytical potential, the potential energy is expressed in the form of a certain known function of atomic coordinates. In the basic case,

a: Institute of High-Temperature Electrochemistry, Ekaterinburg 620066, Russia

* Corresponding author: dmitryz.ihte@gmail.com

this function defines pair interactions and therefore depends on interionic distance only.

The *ab initio* methods imply some approximations to solve the quantum electron equations [1, 2]. Density functional theory (DFT) [2–5] is most commonly used to model molten salts due to the reasonable compromise between computational speed and accuracy. Usually, the Born-Oppenheimer approximation is used, where the coordinates of the nuclei enter the quantum equations as parameters. The *ab initio* molecular dynamics is getting popular year by year due to its accuracy and versatility.

In recent years, a new actor named the Machine Learning Potentials (MLPs) has appeared on the scene of the computational chemistry. Under this joint name, methods for calculating energy and forces are combined, which are based on machine learning methods. MLPs mimic the *ab initio* reference theory to match the *ab initio* accuracy without involving time-consuming quantum chemistry protocols. A comprehensive review on the subject can be found in [6]. One of the popular ML methods is the Behler-Parrinello approach [7, 8]. Here, the total energy is decomposed into the sum of atomic

contributions, which should be calculated by the artificial neural network (ANN) with the input vector composed of so-called symmetry functions describing the local environment.

It should be noted that none of the above-mentioned methods is truly versatile. The ab initio molecular dynamics (AIMD) method makes it possible to simulate melts with minimal empirical information needed and, in theory, to obtain extensive and accurate property data. In practice, however, the limiting factor is the computational complexity of such calculations. AIMD allow simulating ensembles of hundreds of heavy atoms for up to 10^{-10} s (hundreds of picoseconds). The calculation of transport properties requires long time intervals sometimes combined with large ensembles which is not possible to implement within the *ab initio* methods.

Employing the machine learning potentials could partially overcome the disadvantages of AIMD. An increase in the size of the system and time scales available for modeling compared to the reference method makes it possible to obtain qualitatively new data with an accuracy that significantly exceeds the accuracy of model calculations in the framework of classical molecular dynamics. However, the speed of calculations is still much slower as compared to the analytical potentials.

The classical molecular dynamics can operate with ensembles of millions of particles, while the available simulation time, depending on the system, ranges from 10^{-9} to 10^{-6} s. The prediction of numerous properties such as viscosity, electrical conductivity, thermal conductivity, self-diffusion coefficients requires long time runs and/or large ensembles and is therefore beyond the capabilities of AIMD. However, the weak point here is the loss in accuracy of the obtained properties. To a large extent, the performance is defined by the potential applied. Hence, the development and enhancement of classical potentials remains a relevant task.

In this review, we provide a brief description of the protocols for fitting the classical pair potentials.

2. General review of the classical potentials

Within the concept of analytical potential, the potential energy is expressed in the form of a certain known function of atomic coordinates. In the basic case, this function defines pair interaction and therefore depends on the interionic distance. To describe interactions in an ionic liquid using the pair potential approximation, it is necessary to take into account at least two contributions to the pair energy: the long-range Coulomb interaction and the short-range repulsion. The latter is often written in the exponential form:

$$E(r_{ij}) = \frac{q_i q_j}{r_{ij}} + A \cdot \exp\left(\frac{-r_{ij}}{\rho}\right) \qquad (1)$$

Here q_i and q_j are ionic charges, and r_{ij} is the interionic distance. A and ρ are the adjustable parameters of the short-range repulsion term. Some methods for fitting these parameters are discussed in Section 2.1.2. Despite this potential, which is called the Born-Meyer potential, is relatively rarely used, it has been applied in some non-trivial cases such as the calculation of the properties of molten alkali carbonates [9–11], where it showed a controversial performance. Namely, while the density and the thermal expansion coefficient agree well with the experimental data, the calculated thermal conductivity and viscosity are poorly reproduced. However, the performance of the model largely depends on both the potential expression and the fitting procedure. Therefore, a general conclusion on the applicability of the Born-Mayer potential for molten salts cannot be stated so far.

More often, a refined version of the potential is used, which takes into account the dipole-dipole and dipole-quadrupole interactions:

$$E(r_{ij}) = \frac{q_i q_j}{r_{ij}} + A \cdot \exp\left(\frac{-r_{ij}}{\rho}\right) - \frac{C}{r_{ij}^6} - \frac{D}{r_{ij}^8} \qquad (2)$$

In this case, the adjustable parameters of the dispersion terms are C and D. In some scenarios, the ionic charges are the fitting parameters as well [12, 13]. The potential (2) is called the Born-Mayer-Huggins potential. It is widely used to calculate the physicochemical properties of melts [14–20]. The range of simulated systems includes the melts containing multiply charged metal ions and oxygen, which is especially important for industrial applications. Interaction models (1) and (2) imply that the distribution of electron density of the ion does not depend on the instantaneous environment of this ion; such models are the rigid ion models (RIM). For a more plausible description of ions in a melt, an important improvement is the direct consideration of the electron density deformation caused by the local environment. Such models have been developed [21, 22], generally called the polarizable ion models (PIM). Details of the PIM expressions and the parameter fitting procedure are presented elsewhere [22]. It is important to note that the parameters for the PIM are obtained by fitting the model data to those obtained *ab initio*. Not surprisingly, PIM generally outperforms RIM in terms of accuracy [19, 23]. However, the improvement can be insignificant [23–26]. Moreover, for some properties, the results obtained with RIM may be in better agreement with the experimental data. Therefore, a strong accuracy improvement for PIM over RIM cannot be stated in all the cases. The

performance of both PIM and RIM largely depends on the fitting procedure. Below, such a procedure will be discussed for the Born-Mayer potential (1).

3. Numerical fitting of potentials

Let us consider the algorithm of obtaining parameters for the Born-Meyer potential (1), the simplest potential suitable for describing molten salts. The general aim of fitting the parameters of a pair model is to minimize the error function with respect to the parameters P:

$$\Delta(P) \xrightarrow{P} \min \qquad (3)$$

For the Born-Mayer potential, the parameter list consists of the short-range repulsive parameters A and ρ:

$$P = \{A, \rho\} \qquad (4)$$

The error function determines the amount of discrepancy between the data obtained using the pair potential (X^{PP}) and the reference data (X^{ref}). For example, it can be written as:

$$\Delta = \sum_{i=1}^{N} w_i \cdot \left(X_i^{PP} - X_i^{ref} \right)^2 \qquad (5)$$

Here, i index various computing properties. The reference dataset can include information on both microscopic characteristics (potential energies and per-atomic forces) and macroscopic physicochemical properties. In the latter case, it is possible to use experimental data; precise microscopic characteristics are usually available from the *ab initio* calculations only. The priority of the data in the fitting procedure can be adjusted by setting the weight coefficients w_i. In the general case, the error function depends not on two parameters of the potential (1), but on two arrays of parameters:

$$A = \{A_{\alpha\beta}\}$$
$$\rho = \{\rho_{\alpha\beta}\} \qquad (6)$$

Here α and β number the ion types, presented in the system(s) under study. For alkali halides MX (M = Li, Na, K, Rb, Cs; X = F, Cl, Br I) and their mixtures, the total set of parameters is dozens of values. Finding the minimum of an error function over such a large number of variables is a serious challenge. The main difficulties are possible local minima and large computation time (especially when physicochemical properties are calculated). Therefore, for such a wide class of systems, it is reasonable to reduce the problem to an independent fitting of the coefficients for each pair. In this case, the number of parameters to be minimized is two. However, now only pair energies and per-atomic forces are available as reference data. Another drawback of this approach is that the influence of the environment is not taken into account, since the ion pair is considered isolated.

The study [27] describes the process of fitting parameters A and ρ for alkali halides. The reference data were presented by the energies of ion pairs calculated within the framework of the second-order Möller-Plesset perturbation theory (MP2) [28]. The algorithm consisted of two steps. First, the MP2 method was used to calculate the energy of ion pairs depending on the distance between the ions. The total charge of the system was equal to the sum of the oxidation states of the ions. Particular attention was paid to the description of the potential well for the cation-anion pairs. Then, the pair potential (1) was fitted to the obtained discrete dependence. The error function in this case can be proposed as $\Delta = 1 - R^2$, where R^2 is the adjusted R-squared of model predictions. Note that the approximation used (1) is rather rough and for some pairs it gives a noticeable discrepancy between the reference and model energy profiles. Figure 1 shows the dependences of the energy on the distance between Li$^+$ and Cl$^-$ ions. *Ab initio* data are shown as dots while the fitted potential is shown as a solid line. The adjusted R-squared for this pair is equal to 0.9911.

Fitting the pair energy of the Born-Huggins-Mayer potential (2) has some pitfalls due to the presence of several adjustable terms. Technically, *ab initio* data should be better reproduced by the model potential with the additional dispersion terms. However, a reduction in the error function could occur not due to the correct consideration of dispersion interactions, but due to a more flexible functional form. When using a pure mathematical fitting algorithm that knows nothing about underlying chemistry, there is a risk of obtaining unrealistic results. We recommend including physicochemical properties in the error function when fitting the Born-Huggins-Meyer potential.
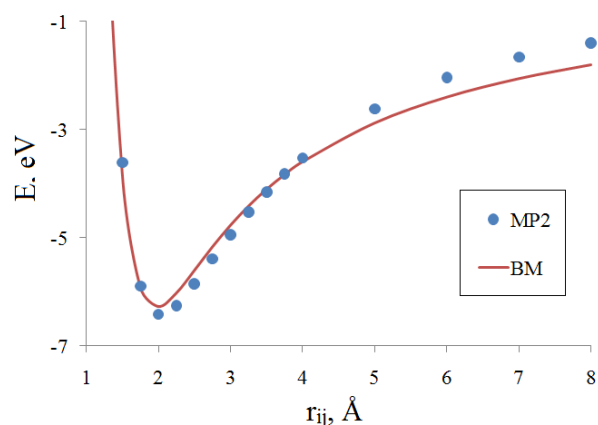

Figure 1 Fitting the Born-Mayer (BM) potential to the *ab initio*-obtained energy [25]. The case of Li$^+$-Cl$^-$ pair.

4. An example: alkali halides

In this section, the potentials for the simulation of alkali halides are discussed. The applied calculations are performed to reveal the impact of the pair potential fitting procedure on potential accuracy. As an example system, molten LiCl is used.

4.1. Simulations of the alkali halides

Molten alkali halides and their mixtures are one of the most studied classes of molten salts. Early (and many subsequent) theoretical investigations used the rigid ion model and the Born-Mayer-Huggins potential (2). The short-range repulsion parameters were obtained by Fumi and Tosi [29] based on the crystallographic data, while the dispersion parameters were obtained by Mayer from the ultraviolet absorption experiments [30]. This approximation dominated for a long time, although various attempts were made to revise the model [31, 32]. In general, the accuracy of calculations strongly depends on the specific properties and composition of the system. However, one can note the general feature of density underestimation when using the Born-Mayer-Huggins-Fumi-Tosi (BMHFT) potential [19, 23, 33, 34]. The assessment of the many-body polarization effects in the form of the PIM could improve the density calculations by a large margin [23]. However, PIM (compared to RIM) do not bring significant advantage in accuracy of alkali halides properties in general [23, 25, 26]. Precise *ab initio* methods are rather costly in calculations and therefore allow obtaining mainly structural information. A significant number of physicochemical properties of interest for practical applications are beyond the scope of AIMD. Recently, the need for accurate physicochemical properties of alkali halides is pushing the utilization of machine learning techniques to drive the molecular dynamics [35–39].

4.2. Fitting the pair potential

As mentioned above, the quality of the potential depends significantly on the way the potential is fitted. Let us support this statement with an example of LiCl. We will consider three pair potentials:

1) The Born-Mayer-Huggins potential (2), parameterized by Fumy, Tosi and Mayer on the basis of experimental data [29, 30]. Hereinafter, this potential is referred to as BMHFT.

2) The Born-Mayer potential (1) parameterized on the basis of the ion pair energies obtained *ab initio* [27]. The detailed information on the fitting methodology is given in Section 3. Hereinafter, this potential is denoted as pair-based Born-Mayer (PBBM).

3) The Born-Mayer potential (1) parameterized through the fitting to the *ab initio* energies of the ion cluster; hereinafter referred to as cluster-based Born-Mayer (CBBM). The details of the fitting procedure are described below.

The consideration of only two ions when obtaining reference energies, as done in [25], does not allow taking into account the effect of the ion's environment in the melt. Although the method based on pair energies produces reasonable potentials, it is reasonable to increase the size of the reference system up to a small cluster of ions. In this case, many-body interactions will be *implicitly* taken into account in the fitting process. Therefore, the performance of the pair potential should improve.

The dataset of fitting data represents a set of "coordinates → energy" records, where the energies of an ion cluster with given ion coordinates are calculated by the precise *ab initio* method. To obtain such a dataset, the *ab initio* molecular dynamics of a $Li_{10}Cl_{10}$ cluster was performed. No periodic boundary conditions were applied; i.e. the considered cluster was isolated. The fitting dataset should include some non-optimal configurations for better quality of the resulting pair potential. Therefore, the temperature was set to 5000 K using the Nose-Hoover thermostat [40] with a time constant of 10 fs. To avoid boiling, harmonic repulsive walls were defined around the system with a cell length being 12 Å. The density functional theory with the PBE0 potential [41] was used. The dispersion correction D3 [42] was applied. The length of the molecular dynamic run was 200 time steps with the each time step being 2 fs. Calculations were performed in the ORCA program [43]. As a result, a set of 200 reference energies was obtained.

To fit the CBBM potential, the gradient descent method was used. The comprehensive review of fitting methods is provided by Martinez et al. [44]. As the starting parameters for optimization, the parameters of the PBBM potential were chosen.

4.3. Testing and comparing the pair potentials

We found that the Li^+-Li^+ and Cl^--Cl^- pair energies vary only slightly for the BMHFT, PBBM, and CBBM potentials, while the Li^+-Cl^- pair potential undergoes the major changes. The comparison of the Li^+-Cl^- pair potentials is presented in Figure 2.

It can be seen that in the BMHFT → PBBM → CBBM row, the position of the minimum shifts towards a larger interionic distance. In addition, the cluster-based fitting (CBBM) resulted in a decrease in the well depth by about 0.3 eV compared to BMHFT and PBBM.

For all three considered potentials (BMHFT, PBBM, and CBBM), molecular dynamics simulations were

performed in the NVE ensemble (constants are the number of particles, the volume, and the total energy) at equilibrium density. The average temperature in all calculations was about 1000 K. The size of the ensembles was 120 ions (60 Li$^+$ + 60 Cl$^-$) which were placed in a cubic cell under periodic boundary conditions. The calculations were carried out using the LAMMPS program [45]. The duration of the simulation run was 10000 time steps, with a time step size of 1 fs. The coordinates of the ions were recorded every 100 time steps to form a set of 100 configurations for each potential. To determine the quality of the potentials, the comparison of the potential energy and the per-atomic forces with the reference data were performed. The reference energy and the forces were calculated by means of the DFT with the Perdew-Burke-Ernzerhof [46] functional. The atoms were described through the split-valence double zeta plus polarization (DZVP) basis sets combined with the Goedecker-Teter-Hutter pseudopotentials [47]. The *ab initio* calculations were performed using the cp2k [48] software package.

The quality of potentials in terms of potential energies and per-atomic forces is illustrated in Figure 3. In this case, the "quality" should be interpreted as "the agreement with the reference *ab initio* method". It is important to note that this agreement does not guarantee a high accuracy in terms of properties calculation. The pale lines represent the perfect $y(x) = x$ function, while the dark lines are the linear fittings of the data. For ease of representation the forces were calculated at the last timestep only. As one can see, the BMHFT potential is struggling to reproduce both DFT energies and DFT forces. Also, this pair potential gives the average values of energies and forces lower by 45–46 %, as compared to the DFT; although the strong conclusion here is barely possible due to the large spread of the data. Switching to the PBBM potential improves the agreement sufficiently, especially in terms of the forces.
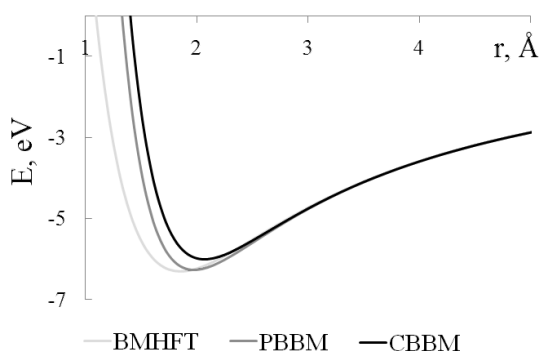

Figure 2 The comparison of the Li$^+$-Cl$^-$ potentials.

Table 1 – Mean absolute errors.

	BMHFT	PBBM	CBBM
Energy, eV	0.574	0.482	0.296
Energy*, meV/ion	4.78	4.02	2.47
Force, eV/Å	0.313	0.206	0.133

* given there are 120 ions in the cell

Nevertheless, the energies obtained by PBBM are 16 % lower than those calculated by the *ab initio* method, which is a significant enhancement over the BMHFT potential.

Finally, the CBBM potential shows the best agreement with the reference DFT method. The energies are slightly overestimated by ~6 %, while the forces have relatively small deviations from the perfect $y(x) = x$ function.

The mean absolute errors (MAEs) of all potentials are summarized in Table 1. It is worth noting that per-atomic energy MAE is less representative since per-atomic errors in energy could cancel out each other.

The comparison with the accurate *ab initio* theory shows that the CBBM potential appears to be the most reliable. This is not surprising, since the fitting in this case was carried out for a system of many ions, which is closer to the melt than the pair approximation (the case of PBBM). In general, it can be recommended to choose a reference system as close as possible to the system that will be the object of study.

4.4. Calculation of properties

To reveal the accuracy of the discussed LiCl potentials in terms of properties calculations, the melting temperature and viscosity were obtained. The melting temperature is one of the most challenging properties to compute even for alkali halides [49]. Obtaining the viscosity requires long simulation runs and therefore employs the strengths of the classical molecular dynamics.

To calculate the melting temperature, the coexisting solid and molten lithium chloride were simulated with the constant enthalpy and pressure of 1 bar. The total number of ions was 3880. The simulation timestep was 0.2 fs to ensure energy conservation. The calculated melting temperature was equal to the equilibrium temperature of the coexisting phases. For BMHFT, PBBM and CBBM the obtained melting temperature was 708, 891 and 952 K, respectively. The experimental value is 883 K [50]. The pair-based Born-Mayer potential gives a quite accurate value with the absolute error being less than 1 %.
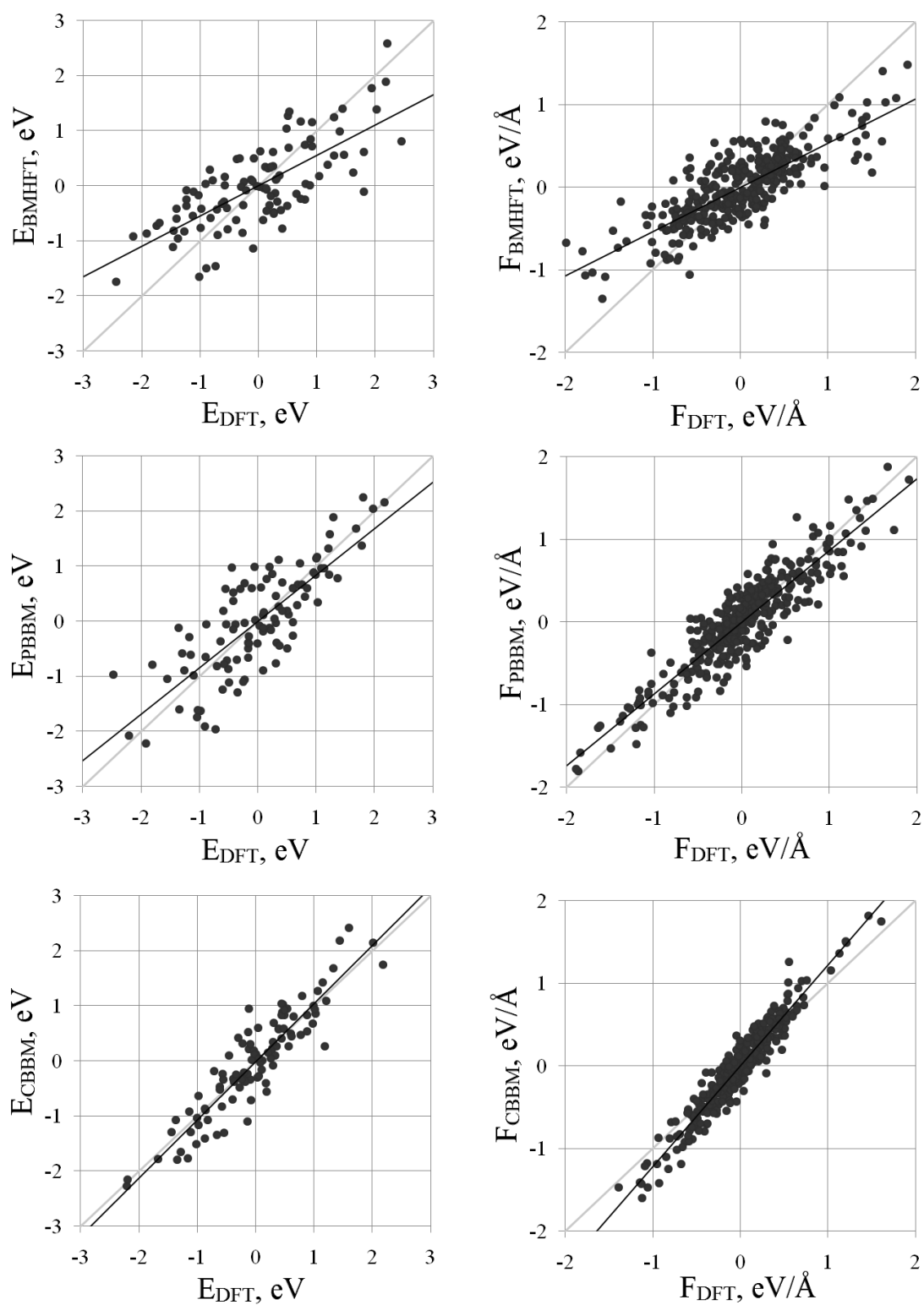
Figure 3 The accuracy of the BMHFT, PBBM and CBBM potentials for calculation of potential energy (left side) and per-atomic forces (right side). As a reference data, the DFT calculation results are taken. Pale lines represent $y(x) = x$ function of a perfect fit. Dark lines are the linear fitting of the obtained data.
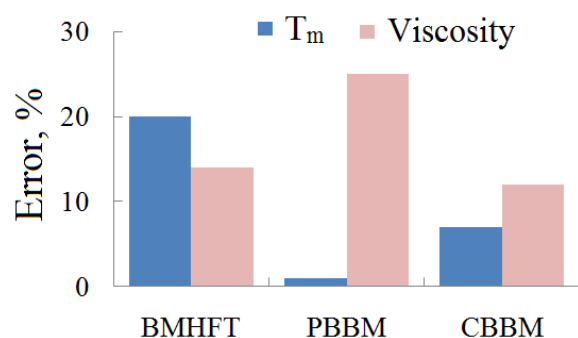
Figure 4 The accuracy of the potentials in terms of properties calculation.

CBBM show an error of 7 %, while the potential parameterized by Fumi and Tosi gives the value that is 20 % lower than the experimental one. These results show that the melting temperature is quite sensitive to the chosen potential.

The viscosity of the melt was calculated under constant energy and volume using the formula (7) [51].

$$\eta = \frac{V}{k_B T} \int_0^{\tau \to \infty} \left\langle \sigma_{\alpha\beta}(t) \cdot \sigma_{\alpha\beta}(0) \right\rangle dt \qquad (7)$$

Here σ is the virial pressure tensor, V is the volume, k_B is the Boltzmann constant, τ is the simulation time. The simulation run length was 100 000 000 steps with a time step of 0.2 fs. The error associated with the time limit can be estimated as 4 %. The registered temperature was about 1000 K. The viscosity values obtained by BMHFT, PBBM and CBBM are 0.928, 1.353 and 1.213 mPa·s, respectively, while the experimental one is 1.082 ± 1 % mPa·s (T = 1000 K) [52]. Therefore, the absolute errors for BMHFT, PBBM and CBBM are 14 %, 25 % and 12 %, respectively. In contrast to the melting temperature calculation, the pair-based Born-Mayer potential shows here the worst agreement with the experimental data, while CBBM shows the best.

The summary of potential accuracy in terms of properties is given in Figure 4. It should be concluded that the accuracy depends on the particular property. Among the potentials considered, the most balanced performance is provided by the cluster-based Born-Mayer potential. This supports the choice of the corresponding reference system in the fitting process.

5. Conclusions

In this paper, the basics of fitting the potentials for molten salts were considered. An analysis of the literature data and practical calculations shows that the procedure for fitting the parameters of the pair potential is no less important than the analytical formula for calculating the energy itself. Using LiCl as an illustrative example, it was shown how the choice of a reference system affects the

accuracy of the pair potential. The comparison of energies and per-atomic forces with those computed *ab initio* shows that the cluster-based potential is the most accurate. Unsurprisingly, this potential delivers the best agreement in terms of macroscopic properties as well, as demonstrated by the examples of melting temperature and viscosity. These results prove that the appropriate fitting procedure could improve the accuracy of the potential to a large extent.

Supplementary materials

No supplementary materials are available.

Funding

Acknowledgments

Author contributions

Dmitry Zakiryanov: Conceptualization, Investigation, Writing – original draft.

Conflict of interest

The authors declare no conflict of interest.

References

1. Pople JA, Nobel Lecture: Quantum chemical models, Rev. Mod. Phys. **71** (1999) 1267–1274. https://doi.org/10.1103/revmodphys.71.1267

2. Geerlings P, De Proft F, Langenaeker W, Conceptual Density Functional Theory, Chem. Rev. **103** (2003) 1793–1874. https://doi.org/10.1021/cr990029p

3. Hohenberg, P, Kohn W, Inhomogeneous Electron Gas, Phys. Rev. **136** (1964) B864–71. https://doi.org/10.1103/physrev.136.b864

4. Kohn W, Sham LJ, Self-Consistent Equations Including Exchange and Correlation Effects, Phys. Rev. **140** (1965) A1133–A1138. https://doi.org/10.1103/physrev.140.a1133

5. Cohen AJ, Mori-Sánchez P, Yang W, Challenges for Density Functional Theory, Chem. Rev. **112** (2011) 289–320. https://doi.org/10.1021/cr200107z

6. Fedik N, Zubatyuk R, Kulichenko M, Lubbers N, et al., Extending machine learning beyond interatomic potentials for predicting molecular properties, Nat. Rev. Chem. **6** (2022) 653–672. https://doi.org/10.1038/s41570-022-00416-3

7. Behler J, Parrinello M, Generalized Neural-Network Representation of High-Dimensional Potential-Energy Surfaces, Phys. Rev. Lett. **98** (2007) 146401. https://doi.org/10.1103/physrevlett.98.146401

8. Behler J, Constructing high-dimensional neural network potentials: A tutorial review, Int. J. Quantum Chem. 115 (2015) 1032–1050. https://doi.org/10.1002/qua.24890

9. Tissen JTWM., Janssen GJM., Molecular-dynamics simulation of molten alkali carbonates, Mol. Phys. 71 (1990) 413–426. https://doi.org/10.1080/00268979000101871

10. Ding J, Du L, Pan G, Lu J, et al., Molecular dynamics simulations of the local structures and thermodynamic properties on molten alkali carbonate K2CO3, Appl. Energy. 220 (2018) 536–544. https://doi.org/10.1016/j.apenergy.2018.03.116

11. Du L, Xie W, Ding J, Lu J, et al., Molecular dynamics simulations of the thermodynamic properties and local structures on molten alkali carbonate Na2CO3, Int. J. Heat Mass Transf. 131 (2019) 41–51. https://doi.org/10.1016/j.ijheatmasstransfer.2018.11.044

12. Seo W-G, Matsuura H, Tsukihashi F, Calculation of phase diagrams for the FeCl2, PbCl2, and ZnCl2 binary systems by using molecular dynamics simulation, Metall. Mater. Trans. B 37 (2006) 239–251. https://doi.org/10.1007/bf02693154

13. Lee S-C, Zhai Y, Li Z, Walter NP, et al., Comparative Studies of the Structural and Transport Properties of Molten Salt FLiNaK Using the Machine-Learned Neural Network and Reparametrized Classical Forcefields, J. Phys. Chem. B. 125 (2021) 10562–10570. https://doi.org/10.1021/acs.jpcb.1c05608

14. Galamba N, Nieto de Castro CA, Ely JF, Molecular Dynamics Simulation of the Shear Viscosity of Molten Alkali Halides, J. Phys. Chem. B. 108 (2004) 3658–3662. https://doi.org/10.1021/jp036234x

15. Galamba N, Nieto de Castro CA, Ely JF, Thermal conductivity of molten alkali halides from equilibrium molecular dynamics simulations, Chem. Phys. 120 (2004) 8676–8682. https://doi.org/10.1063/1.1691735

16. Galamba N, Nieto de Castro CA, Ely JF, Shear viscosity of molten alkali halides from equilibrium and nonequilibrium molecular-dynamics simulations, Chem. Phys. 122 (2005) 224501. https://doi.org/10.1063/1.1924706

17. Wang J, Sun Z, Lu G, Yu J, Molecular Dynamics Simulations of the Local Structures and Transport Coefficients of Molten Alkali Chlorides, J. Phys. Chem. B. 118 (2014) 10196–10206. https://doi.org/10.1021/jp5050332

18. Zhang S, Jin Y, Yan Y, Depression of melting point and latent heat of molten salts as inorganic phase change material: Size effect and mechanism, J. Mol. Liq. 346 (2022) 117058. https://doi.org/10.1016/j.molliq.2021.117058

19. Wu J, Ni H, Liang W, Lu G, et al., Molecular dynamics simulation on local structure and thermodynamic properties of molten ternary chlorides systems for thermal energy storage, Comput. Mater. Sci. 170 (2019) 109051. https://doi.org/10.1016/j.commatsci.2019.05.049

20. Lv X, Dong A, Dai Y, Wang J et al., Temperature and concentration dependence of the physical properties and local structures of molten NaCl-KCl-LiCl mixtures, J. Mol. Liq. 229 (2017) 330–338. https://doi.org/10.1016/j.molliq.2016.12.091

21. Salanne M, Madden PA, Polarization effects in ionic solids and melts, Mol. Phys. 109 (2011) 2299–2315. https://doi.org/10.1080/00268976.2011.617523

22. Salanne M, Rotenberg B, Jahn S, Vuilleumier R, et al., Including many-body effects in models for ionic liquids, Theor. Chem. Acc. 131 (2012). https://doi.org/10.1007/s00214-012-1143-9

23. Wang H, DeFever RS, Zhang Y, Wu F, et al., Comparison of fixed charge and polarizable models for predicting the structural, thermodynamic, and transport properties of molten alkali chlorides, Chem. Phys. 153 (2020) 214502. https://doi.org/10.1063/5.0023225

24. Takagi R, Hutchinson F, Madden PA, Adya AK, et al., The structure of molten and simulated with polarizable- and rigid-ion models, J. Phys. Condens. Matter 11 (1999) 645–658. https://doi.org/10.1088/0953-8984/11/3/00

25. Ishii Y, Kasai S, Salanne M, Ohtori N, Transport coefficients and the Stokes–Einstein relation in molten alkali halides with polarisable ion model, Mol. Phys. 113 (2015) 2442–2450. https://doi.org/10.1080/00268976.2015.1046527

26. DeFever RS, Wang H, Zhang Y, Maginn EJ, Melting points of alkali chlorides evaluated for a polarizable and non-polarizable model, J. Chem. Phys. 153 (2020) 011101. https://doi.org/10.1063/5.0012253

27. Zakiryanov D, Kobelev M, Tkachev N, Melting properties of alkali halides and the cation-anion size difference: A molecular dynamics study, Fluid Ph. Equilibria. 506 (2020) 112369. https://doi.org/10.1016/j.fluid.2019.112369

28. Møller C, Plesset MS, Note on an Approximation Treatment for Many-Electron Systems, Phys. Rev. 46 (1934) 618–622. https://doi.org/10.1103/physrev.46.618

29. Tosi MP, Fumi FG, Ionic sizes and born repulsive parameters in the NaCl-type alkali halides—II, J. Phys. Chem. Solids 25 (1964) 45–52. https://doi.org/10.1016/0022-3697(64)90160-x

30. Mayer JE, Dispersion and Polarizability and the van der Waals Potential in the Alkali Halides, Chem. Phys. 1 (1933) 270–279. https://doi.org/10.1063/1.1749283

31. Woodcock LV, Interionic pair potentials in the alkali metal halides, J. Chem. Soc. Faraday Trans. 70 (1974) 1405. https://doi.org/10.1039/f29747001405

32. Michielsen J, Woerlee P, v.d. Graaf F, Ketelaar JAA, Pair potential for alkali metal halides with rock salt crystal structure. Molecular Dynamics Calculations on NaCl and LiI, J. Chem. Soc. Faraday Trans. 71 (1975) 1730. https://doi.org/10.1039/f29757101730

33. Pan G-C, Ding J, Wang W, Lu J, et al., Molecular simulations of the thermal and transport properties of alkali chloride salts for high-temperature thermal energy storage, Int. J. Heat Mass Transf. 103 (2016) 417–427. https://doi.org/10.1016/j.ijheatmasstransfer.2016.07.042

34. Wang J, Wu J, Sun Z, Lu G, et al., Molecular dynamics study of the transport properties and local structures of molten binary systems (Li, Na)Cl, (Li, K)Cl and (Na, K)Cl, J. Mol. Liq. **209** (2015) 498–507. https://doi.org/10.1016/j.molliq.2015.06.021

35. Sivaraman G, Guo J, Ward L, Hoyt N, et al., Automated Development of Molten Salt Machine Learning Potentials: Application to LiCl, J. Phys. Chem. Lett. **12** (2021) 4278–4285. https://doi.org/10.1021/acs.jpclett.1c00901

36. Lee S-C, Zhai Y, Li Z, Walter NP, et al., Comparative Studies of the Structural and Transport Properties of Molten Salt FLiNaK Using the Machine-Learned Neural Network and Reparametrized Classical Forcefields, J. Phys. Chem. B **125** (2021) 10562–10570. https://doi.org/10.1021/acs.jpcb.1c05608

37. Tovey S, Narayanan Krishnamoorthy A, Sivaraman G, Guo J, et al., DFT Accurate Interatomic Potential for Molten NaCl from Machine Learning, J. Phys. Chem. C. **124** (2020) 25760–25768. https://doi.org/10.1021/acs.jpcc.0c08870

38. Rodriguez A, Lam S, Hu M, Thermodynamic and Transport Properties of LiF and FLiBe Molten Salts with Deep Learning Potentials, ACS Appl. Mater. Interfaces **13** (2021) 55367–55379. https://doi.org/10.1021/acsami.1c17942

39. Guo J, Ward L, Babuji Y, Hoyt N, et al., Composition-transferable machine learning potential for LiCl-KCl molten salts validated by high-energy x-ray diffraction, Phys. Rev. B. **106** (2022). https://doi.org/10.1103/physrevb.106.014209

40. Nosé S, A unified formulation of the constant temperature molecular dynamics methods, Chem. Phys. **81** (1984) 511–519. https://doi.org/10.1063/1.447334

41. Adamo C, Barone V, Toward reliable density functional methods without adjustable parameters: The PBE0 model, Chem. Phys. **110** (1999) 6158–6170. https://doi.org/10.1063/1.478522

42. Grimme S, Antony J, Ehrlich S, Krieg H, A consistent and accurate ab initio parametrization of density functional dispersion correction (DFT-D) for the 94 elements H-Pu, Chem. Phys. **132** (2010) 154104. https://doi.org/10.1063/1.3382344

43. Neese F, The ORCA program system, Wiley Interdiscip. Rev. Comput. Mol. Sci. **2** (2011) 73–78. https://doi.org/10.1002/wcms.81

44. Martinez JA, Yilmaz DE, Liang T, Sinnott SB et al., Fitting empirical potentials: Challenges and methodologies, Curr. Opin. Solid State Mater. Sci. **17** (2013) 263–270. https://doi.org/10.1016/j.cossms.2013.09.001

45. Plimpton S, Fast Parallel Algorithms for Short-Range Molecular Dynamics, J. Comput. Phys. **117** (1995) 1–19. https://doi.org/10.1006/jcph.1995.1039

46. Perdew JP, Burke K, Ernzerhof M, Generalized Gradient Approximation Made Simple, Phys. Rev. Lett. **77** (1996) 3865–3868. https://doi.org/10.1103/physrevlett.77.3865

47. Goedecker S, Teter M, Hutter J, Separable dual-space Gaussian pseudopotentials, Phys. Rev. B. **54** (1996) 1703–1710. https://doi.org/10.1103/physrevb.54.1703

48. Hutter J, Iannuzzi M, Schiffmann F, Van de Vondele J, cp2k: atomistic simulations of condensed matter systems, Wiley Interdiscip. Rev. Comput. Mol. Sci. **4** (2013) 15–25. https://doi.org/10.1002/wcms.1159

49. Aragones JL, Sanz E, Valeriani C, Vega C, Calculation of the melting point of alkali halides by means of computer simulations, J. Chem. Phys. **137** (2012) 104507. https://doi.org/10.1063/1.4745205

50. Janz GJ, Tomkins RPT. Physical Properties Data Compilations Relevant to Energy Storage. IV. Molten Salts: Data on Additional Single and Multi-Component Salt Systems. U S. Government printing office: Washington; 1981. P. 280.

51. Porter T, Vaka MM, Steenblik P, Della Corte D, Computational methods to simulate molten salt thermophysical properties. Commun. Chem **5** (2022) 69. https://doi.org/10.1038/s42004-022-00684-6

52. Janz GJ. Thermodynamic and Transport Properties for Molten Salts: Correlation Equations for Critically Evaluated Density, Surface Tension, Electrical Conductance, and Viscosity Data (Supplement 2). J. Phys. Chem. Ref. Data **17** (1998).